Biomaterials Science

Dose optimization of decellularized skeletal muscle extracellular matrix hydrogels for improving perfusion and subsequent validation in an aged hindlimb ischemia model

Journal:	*Biomaterials Science*
Manuscript ID	BM-ART-12-2019-001963.R1
Article Type:	Paper
Date Submitted by the Author:	14-Apr-2020
Complete List of Authors:	Hernandez, Melissa; University of California San Diego, Bioengineering Zelus, Emma; University of California San Diego, Bioengineering Spang, Martin; University of California San Diego, Bioengineering Braden, Rebecca; University of California San Diego, Bioengineering Christman, Karen; University of California San Diego, Bioengineering

PAPER

Dose optimization of decellularized skeletal muscle extracellular matrix hydrogels for improving perfusion and subsequent validation in an aged hindlimb ischemia model

Received 00th December 2019,
Accepted 00th January 20xx

DOI: 10.1039/x0xx00000x

Melissa J. Hernandez, Emma I. Zelus, Martin T. Spang, Rebecca L. Braden, and Karen L. Christman*

Peripheral artery disease (PAD) affects more than 27 million individuals in North America and Europe, and current treatment strategies mainly aim to restore blood perfusion. However, many patients are ineligible for existing procedures, and these therapies are often ineffective. Previous studies have demonstrated success of an injectable decellularized skeletal muscle extracellular matrix (ECM) hydrogel in a young rat hindlimb ischemia model of PAD, but further pre-clinical studies are necessary prior to clinical translation. In this study, varying concentrations of a skeletal muscle ECM hydrogel were investigated for material properties and *in vivo* effects on restoring blood perfusion. Rheological measurements indicated an increase in viscosity and mechanical strength with the higher concentrations of the ECM hydrogels. When injecting dye-labelled ECM hydrogels into a healthy rat, differences were also observed for the spreading and degradation rate of the various concentrations. The three concentrations for the ECM hydrogel were then further examined in a young rat hindlimb ischemia model. The efficacy of the optimal ECM hydrogel concentration was then further confirmed in an aged mouse hindlimb ischemia model. These results further validate the use of decellularized skeletal muscle ECM hydrogels for improving blood perfusion in small animal models of PAD.

1. Introduction

Peripheral artery disease (PAD), an ischemic condition caused by atherosclerosis, can be categorized into two main classifications – intermittent claudication and critical limb ischemia (CLI). For individuals with CLI, the more severe form of PAD, patients experience fatigue while at rest, and the lack of blood flow to the skeletal muscle can result in muscle atrophy, muscle fiber loss and damage, denervation, and may necessitate amputation. In fact, amputations become necessary for 120,000 patients in the United States and 100,000 patients in the European Union each year.[1] Current treatment strategies for these patients include endovascular procedures, such as atherectomies or balloon angioplasty with or without stenting, or surgical approaches, like bypass grafting. However, due in part to the diffuse nature of the condition, only 40% of patients are eligible for existing procedures,[2] and restenosis rates may exceed 45% following these interventions.[3]

Many regenerative medicine applications, such as cells and growth factors, have been investigated in Phase I clinical trials, but the majority of these studies have failed. To overcome the challenges associated with treating PAD patients, biomaterials have been investigated as a possible solution.[4,5] Specifically, biomaterial-alone approaches have utilized a decellularized skeletal muscle extracellular matrix (ECM) hydrogel,[6,7] fibrin,[8] and fucoidan.[9] In particular, decellularized ECM has been studied extensively for regenerative medicine applications due to its ability to mimic the biochemical cues of the native ECM[10,11] and its degradation products, which are angiogenic[12] and promote cell migration and proliferation.[12-18] In one study, a decellularized skeletal muscle ECM hydrogel at a concentration of 6 mg/mL demonstrated efficacy in a young rat hindlimb ischemia model of PAD.[7] With a single intramuscular injection of the ECM hydrogel administered one week post-hindlimb ischemia surgery, an increase in blood perfusion relative to a saline control was observed, which was attributed to increases in arteriogenesis.[7]

Although the efficacy of the skeletal muscle ECM hydrogel has been previously shown, an optimal concentration was not investigated. In another study, a higher concentration of the skeletal muscle ECM hydrogel (8 mg/mL) was used to improve cellular retention and survival of myoblasts and fibroblasts in a mouse hindlimb ischemia model, but the higher concentration was not investigated independently of the cells.[19] Altering the material concentration could impact both the density of biochemical cues as well as the physical properties of the material, both of which could impact the biological response. Therefore, determining an optimal concentration of the skeletal muscle ECM hydrogel could be critical for enhancing therapeutic outcomes.

In addition to investigating the efficacy of various concentrations of the ECM hydrogel, it would be advantageous to evaluate these materials further in more representative animal models. Certain risk factors, including age, diabetes, smoking, hypertension, and hypercholesterolemia, lead to an increased prevalence of PAD. Specifically, the prevalence of PAD increases by age group – 1.43% for 40-49 years, 3.41% for 50-59 years, 7.77% for 60-69 years, and 16.62% for 70 years and older.[20] Aging has been shown to impair essential biological processes[21] such as angiogenesis,[22,23]

Department of Bioengineering, Sanford Consortium for Regenerative Medicine, University of California San Diego, 2880 Torrey Pines Scenic Dr., La Jolla, CA, 92037, USA

vasculogenesis,[23] innervation,[24,25] and satellite cell activity[26-28] and may also contribute to increased muscle fibrosis.[27,29,30] However, few studies have assessed therapeutics for PAD in aged animal models,[31-38] with only two of these studies pertaining to biomaterial therapies.[37,38]

Here we performed a dose optimization study with three concentrations (4, 6, and 8 mg/mL) of a decellularized skeletal muscle ECM hydrogel. We evaluated the physical properties of these hydrogels with rheological measurements and imaging of the nanofibrous architectures. In addition, the material retention and *in vivo* spread was evaluated prior to performing hindlimb ischemia surgeries in young rats. The optimal concentration was then validated further in an aged mouse hindlimb ischemia model. These results further demonstrate the translational potential of a decellularized skeletal muscle ECM hydrogel for PAD patients.

2. Materials and methods

All experiments in this study were performed in accordance with the guidelines established by the Institutional Animal Care and Use Committee at the University of California San Diego and the American Association for Accreditation of Laboratory Animal Care. All protocols were approved by the Institutional Animal Care and Use Committee at the University of California San Diego.

2.1 Material processing

Based on previously published protocols,[39,40] longissimus dorsi muscles, commonly known as pork loin, were obtained from Yorkshire farm pigs (4-7 months old, S&S Farms) from the UC San Diego medical school. Briefly, the muscle was harvested, frozen for a minimum of 24 hours, and then chopped into 0.5 cm^3 pieces. Tissue was decellularized for 4-5 days in a solution of 1% wt/vol sodium dodecyl sulfate (SDS) in 1X phosphate buffered saline (PBS) with 10,000 U penicillin/streptomycin (ThermoFisher Scientific, Waltham, MA), placed in isopropanol for 18-24 hours to remove residual lipids, and then rinsed in water for another 24 hours. The tissue was then removed, frozen at -80°C, lyophilized, and milled using a Wiley Mini-Mill (Thomas Scientific, Swedesboro, NJ) with a #60 filter. The milled powder was then partially digested with pepsin (Sigma-Aldrich, St. Louis, MO) in 0.1 M HCl (1 mg/mL) at a final concentration of 10 mg ECM/1 mL pepsin solution for 48 hours. Following digestion, the ECM solution was neutralized to pH 7.4 and adjusted to 1X PBS for 4, 6, and 8 mg/mL concentrations. Aliquots were then lyophilized once more for long-term storage at -80°C.

2.2 Resuspension of ECM hydrogels

Lyophilized aliquots of the decellularized skeletal muscle ECM hydrogels were resuspended to their respective concentrations with deionized (DI) water (i.e. 300 µL DI water for a 2 mg ECM aliquot for 6 mg/mL concentration). The lyophilized particulates were initially broken up by pipetting up and down gently, and the aliquots were then left on ice for ~10 minutes to allow for the material to solubilize. After 10 minutes, the aliquots were fully resuspended by pipetting the mixture until no large particulates remained. A 25G syringe was then used to shear the material further, which ultimately yielded a homogenous liquid.

2.3 Scanning electron microscopy

Prior to performing scanning electron microscopy (SEM), 300 µL of each concentration of the skeletal muscle ECM hydrogels were prepared according to section 2.2. Gels were formed by incubating at 37°C for 24 hours. Each gel was then fixed for 24 hours in an aqueous mixture of EM-grade 4% paraformaldehyde and 4% glutaraldehyde. Following fixation, the gels were then dehydrated with a series of ethanol rinses (30%, 50%, 75%, 90%, and 100%), each one lasting 30 minutes. Once the dehydration was complete, the ethanol was aspirated from the gels, and the gels were suspended in isopropyl alcohol. Fixed and dehydrated hydrogels were then loaded into Teflon sample holders and processed in an AutoSamdri 815A automated critical point drier (Tousimis, Rockville, MD). The protocol included 40 exchange cycles of CO_2 at medium speed and 40% stirring. The fill and heating steps were performed at slow speed, while the venting step was performed at medium speed. Mounted samples were then sputter coated using a Leica EM SCD500 (Leica Microsystems, Wetzlar, Germany) with approximately 7 nm of iridium while being rotated. Representative images of the samples were then taken on a FEI Quanta 250 FEG scanning electron microscope (ThermoFisher Scientific, Waltham, MA) at 3 kV using the in-lens SE1 detector.

2.4 Rheometry

To perform complex viscosity measurements, 200 µL of resuspended ECM was pipetted onto the stage of a parallel plate ARG2 rheometer (TA Instruments, New Castle, DE). With a fixed plate temperature set to 25°C to maintain a liquid solution and the gap height adjusted to 500 µm, a flow procedure was run with shear rates varying from 0.1 to 100 Hz. To ensure delivery via syringe, the materials were assessed for shear thinning properties.

To determine the storage and loss moduli, 500 µL of the ECM mixtures were pipetted into 4 mL scintillation vials and allowed to gel at 37°C for 24 hours. The hydrogels were then carefully removed and placed on the rheometer stage with a fixed plate temperature of 37°C. The gap height was then adjusted to 1100 µm, and an oscillatory sweep run was performed with the frequency ranging from 0.1 to 100 rad/s. Values for the storage and loss moduli were reported at 1 rad/s.

2.5 Animals

For the material retention and dose optimization studies, female Sprague Dawley rats (~10 weeks, Charles River, Wilmington, MA) were used. Male C57BL/6 mice (~32 weeks, Jackson Laboratory, Bar Harbor, ME) were utilized for the aged hindlimb ischemia study. All animals were provided with food and water *ad libitum*.

2.6 Material spreading and retention

An Alexa Fluor™ 568 NHS ester (succinimydl ester) dye was prepared by diluting the lyophilized powder to 10 mg/mL in sterile dimethyl sulfoxide (DMSO), according to a previous study.[41] Sterile ECM aliquots were then resuspended as described in section 2.2. The dye was mixed with the resuspended ECM according to the following ratios to account for the varying ECM protein concentrations: 6.7 µL/1 mL 4 mg/mL ECM, 10 µL dye/1 mL 6 mg/mL ECM, and 13.3 µL/1

mL 8 mg/mL ECM. Once thoroughly mixed by pipetting, the solutions were left on ice in the dark for 1 hour to allow the dye to conjugate to the primary amines of the proteins. Syringes with a 27G needle were prepared with 150 µL of one of the three concentrations and kept in the dark until use.

Healthy rats (n=2/concentration) were anesthetized with isoflurane (VetOne, Boise, ID), and the anterior sides of both hindlimbs were prepared for injections, resulting in n=4 per concentration. While extending the limb with one hand, 150 µL of the ECM hydrogel was injected at a ~30° angle into the middle of the gracilis muscle over approximately 30 seconds. The needle was then held in place for another 15 seconds to prevent the material from leaking out. This injection procedure was repeated for both hindlimbs with the same concentration used on both sides.

At 1 and 2 weeks post-injection, the rats were euthanized with an intraperitoneal injection of 200 mg/kg Fatal-Plus® (Vortech Pharmaceuticals, Dearborn, MI). Both gracilis muscles (n=4/concentration) were harvested and flash frozen in liquid nitrogen-chilled 2-methylbutane. The muscles were then allowed to freeze at -80°C for a minimum of 24 hours before individually embedding the muscles in Tissue-Tek® O.C.T. (Sakura Finetek, Torrance, CA) and once again flash freezing the samples in liquid nitrogen-chilled 2-methylbutane.

Samples were cryosectioned into 10-µm thick sections on a Leica CM3050 S cryostat (Leica Biosystems, Nussloch, Germany). A total of 13 evenly-spaced locations were sampled from the gracilis muscles with 400 µm between locations. One microscope slide from each location was then stained with Hoechst 33342 (1 µL/10 mL DI water, ThermoFisher Scientific, Waltham, MA). Slides were dried overnight before imaging with an Ariol DM6000 B microscope (Leica Microsystems, Wetzlar, Germany). An overview image was captured for each microscope slide, and ImageJ was then used to manually outline the entire tissue section based on the blue channel. The material in the red channel was then individually thresholded for each image, and the areas of the entire tissue section and labelled material were extracted for analysis. A % area value was determined from a ratio of the labelled material area relative to the total tissue section area. Calculations were performed to quantify the amount of the ECM hydrogel at each location and for the entire muscle.

2.7 Hindlimb ischemia surgery

Animals were anesthetized with isoflurane and then placed in a supine position on a DSx vented warming table (VetEquip, Livermore, CA). Prior to beginning the surgery, a subcutaneous injection of 0.05 mg/kg buprenorphine (Pfizer, New York, NY) was administered and a 1% lidocaine (Hospira, Lake Forest, IL) line block was injected along the right hindlimb. In addition, 0.5 mL (mouse) or 3 mL (rat) of lactated ringers (B. Braun Medical, Melsungen, Germany) were administered subcutaneously to keep the animals hydrated. The right hindlimb was shaved and disinfected with Betadine (Purdue Pharma L.P., Stamford, CT) and 70% isopropanol. Sterile saline was used throughout the surgery to keep the tissues from drying out. An incision was made through the skin beginning in the inguinal region and extending along the visible femoral vessels to the branch of the saphenous. Fat in the inguinal regions was cauterized to improve visibility, and the nerve was then carefully dissected from the vessels. A 5-0 Solfsilk suture (Covidien, Dublin, Ireland) was used for permanent occlusion of the arteries and veins. Two ligatures were placed proximal to the branch of the saphenous vessels, one ligature each was placed on the popliteal and genicular vessels, and two ligatures were placed around the lateral circumflex femoral vessels distal to the inguinal ligament. The vessels were carefully transected between the occlusion points, and all other vessels were cauterized as needed. The skin was then closed with 5-0 monocryl (Ethicon, Somerville, NJ) for the mice and 9 mm autoclips (MikRon Precision Inc., Gardena, CA) for the rats. Lastly, another 1% lidocaine line block was injected subcutaneously and triple antibiotic ointment (Activis, Parsipanny-Troy Hills, NJ) was applied. Animals were then immediately transferred for blood perfusion imaging.

2.8 Laser speckle contrast analysis imaging

To monitor the blood perfusion levels in the hindlimbs, laser speckle contrast analysis (LASCA) imaging was utilized.[7,42,43] All recordings were performed with a PeriCam PSI System (Perimed, Stockholm, Sweden) using the following settings: ~20 cm working distance, high point density, 19 images/s frame rate, recorded with averaging of 60 images, and effective frame rate of 0.3 images/s. Animals were anesthetized with isoflurane, transferred to a face mask on a heated deck (Hallowell EMC, Pittsfield, MA) and placed in a prone position. The heated deck ensured consistency of the animals' core temperatures. Prior to beginning a recording, regions of interest (ROIs) were placed around both paws, with particular attention paid to avoid including extra fur with the rats. Imaging was continued until the blood perfusion values plateaued, which typically occurred around 20 minutes. All animals were imaged immediately pre- and post-hindlimb ischemia surgery to ensure the blood perfusion levels in both paws were similar (<30% difference) prior to surgery and to confirm the hindlimb ischemia surgeries decreased the blood perfusion in the right (ischemic) paw. Blood perfusion levels for the rats were recorded on days -2, 7, 21, and 35, and blood perfusion levels for the mice were recorded on days -2, 3, 7, 14, 21, and 28. Additional time points were included for the mouse studies since the timing of the blood perfusion recovery was unknown. All perfusion values are reported relative to the left (healthy) paw.

2.9 Intramuscular injections

One week post-hindlimb ischemia surgery (Day 0), the skeletal muscle ECM hydrogel (n=7 or 8 for rats; n=6 for mice) or saline (n=8 for rats; n=6 for mice) was injected intramuscularly. This delayed injection approach allowed for the initial inflammation from the hindlimb ischemia surgery to resolve before injecting the material. Saline was used as a control to serve as a baseline for any muscle regeneration that may occur as a result of an inflammatory response from the injection itself, whereas collagen hydrogels, another potential control, were previously shown to be less bioactive.[6] Animals were randomized according to day -7 and -2 blood perfusion measurements to ensure no significant differences existed between experimental groups prior to the injection. The ECM hydrogels were resuspended under aseptic conditions as described in section 2.2, and a 27G needle was used for all of the injections. Animals were anesthetized with 5% isoflurane, transferred to a heated deck with a face mask, and then placed in a supine position. For the rats, both

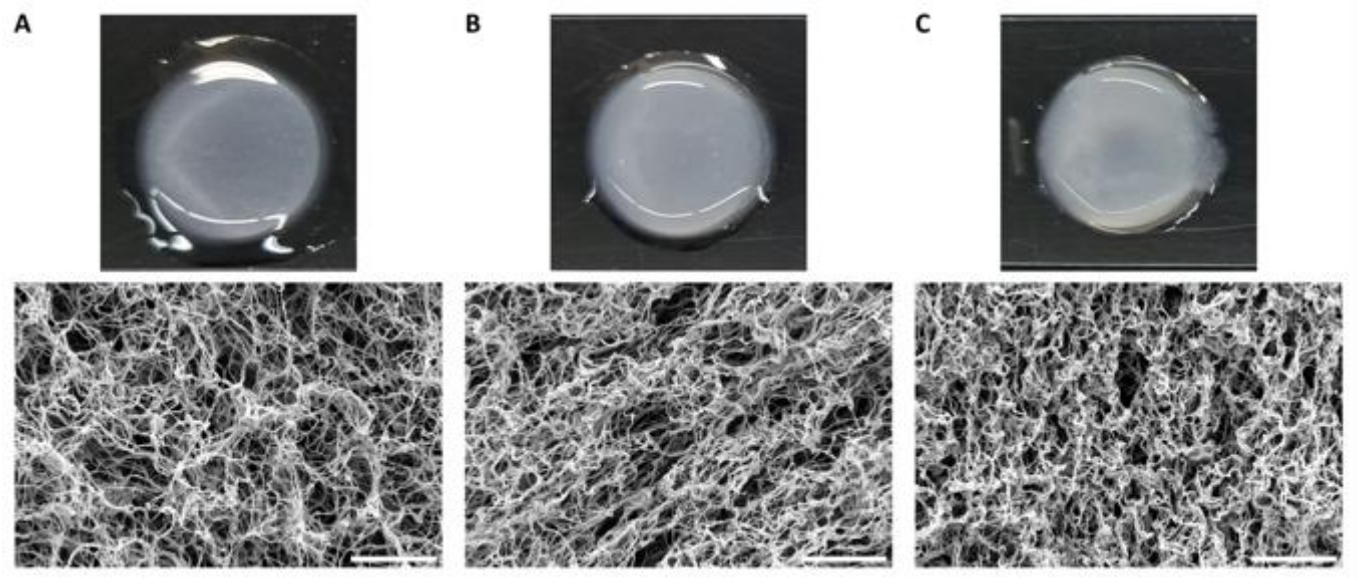

Fig. 1 Structural properties of the three ECM hydrogel concentrations. Hydrogel (top) and scanning electron microscopy images (bottom) of (A) 4 mg/mL, (B) 6 mg/mL, and (C) 8 mg/mL decellularized skeletal muscle ECM hydrogels. Scale bar is 5 μm.

hindlimbs were extended to fully expose the gracilis muscles, the paws were taped down, and any remaining staples were removed from the right (ischemic) hindlimb. The needle was inserted at the medial point of the suture line at a ~30° angle, and 150 μL of saline or ECM were injected into the right (ischemic) gracilis muscle. For the mice, the right paw was held with the knee at a 120° angle, and 25 μL of saline or ECM were injected at a ~15° angle into the tibialis anterior muscle. Material injections were performed over ~30 seconds, and the needle was left in place for ~15 seconds after the injection to ensure material would not leak out.

2.10 Statistical analysis

Results are reported as mean ± SEM. Prism 8 (GraphPad Software, San Diego, CA) was utilized for all statistical analyses. For the mechanical properties and material retention experiments, a one-way ANOVA with a Tukey's post hoc test was used to assess the three ECM hydrogel concentrations. Blood perfusion improvements (day -2 vs. day 35) from the rat hindlimb ischemia study were analyzed with a one-way ANOVA with a Dunnet's post hoc test to allow for comparisons of the mean improvements from each concentration relative to the saline control. The aged mouse hindlimb ischemia study utilized an unpaired Student's t-test for the day 28 perfusion measurements. Significance for all statistical tests was accepted at $p < 0.05$.

3. Results and discussion

3.1 Physical properties

For processing the decellularized skeletal muscle ECM hydrogels, a digestion procedure was used, which was based on an existing protocol for the manufacturing of a decellularized myocardial ECM hydrogel. With this digestion procedure, which is performed at 10 mg/mL, it is difficult to reliably achieve concentrations much higher than 8 mg/mL, and higher concentrations pose difficulties with injecting through high gauge needles. Subcutaneous injections of the ECM hydrogels at concentrations of 2 mg/mL, 4 mg/mL, 6 mg/mL,

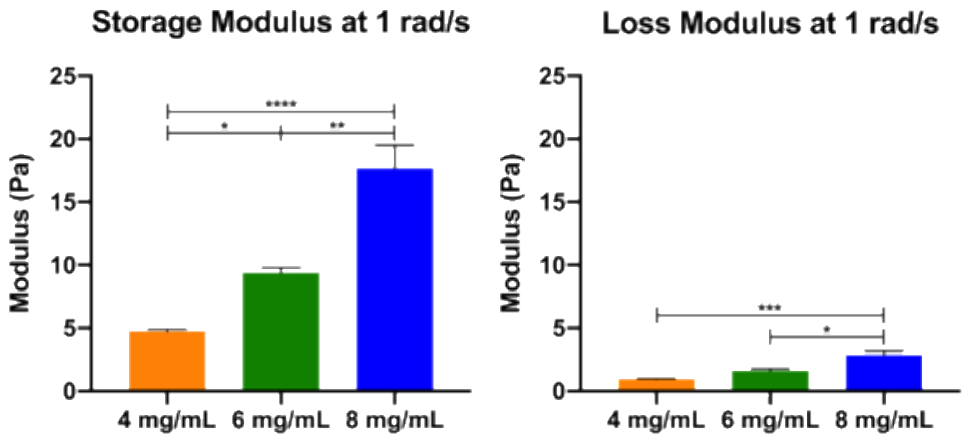

Fig. 2 Storage and loss moduli values increased with the higher concentrations of the ECM hydrogels. *p < 0.05, **p < 0.01, ***p < 0.001, ****p < 0.0001. Data are mean ± SEM.

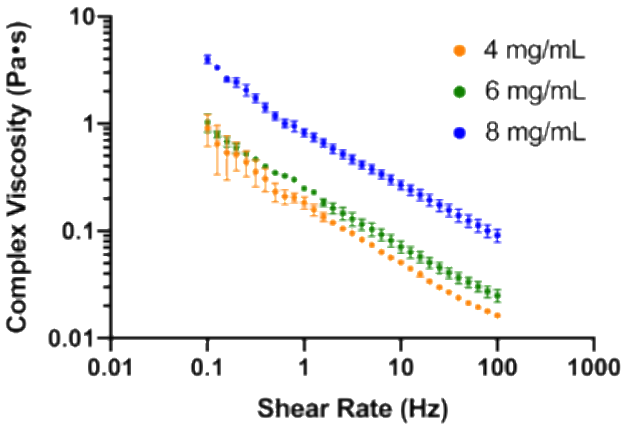

Fig. 3 Viscosity measurements for all three ECM hydrogels demonstrated shear thinning properties. Data are mean ± SEM.

and 8 mg/mL (data not shown) demonstrated that the 2 mg/mL hydrogel did not sufficiently gel and instead diffused quickly following the injection. As a result, only skeletal muscle ECM hydrogels with a concentration of 4 mg/mL, 6 mg/mL, or 8 mg/mL were investigated in this study.

Physical properties and biochemical cues, both of which change with differing concentrations, represent possible mechanisms by which biomaterials may promote regeneration. Therefore, identifying an optimal concentration was necessary to confirm whether various concentrations of an ECM hydrogel impacted *in vivo* efficacy. To first investigate the physical properties of the ECM hydrogels, hydrogels were formed *in vitro* for the three concentrations; the gels became more opaque and less weeping of fluid was observed with increasing concentration (Fig. 1). SEM images were then collected to examine the nanofibrous architecture of the ECM hydrogels (Fig. 1), which was previously shown to only be present after successful gelation.[44] As the concentration of the ECM hydrogels and therefore ECM proteins increased, the proteins became more densely packed together. The fibers in the 4 mg/mL hydrogel were less densely packed, whereas the 8 mg/mL ECM hydrogel was more densely packed, and the nanofibers were more closely aligned. The architecture of the 6 mg/mL ECM hydrogel most closely resembled the 8 mg/mL ECM hydrogel. Since the samples were dehydrated as part of the preparation process for SEM imaging, the ECM proteins likely collapsed to some degree, and, consequently the images cannot fully recapitulate how these hydrogels appear *in vivo*. Nonetheless, it was hypothesized that the increased packing density of the ECM proteins in the higher concentration ECM hydrogels would affect a cell's ability to infiltrate the material and begin remodelling the environment.

The three concentrations of the skeletal muscle ECM hydrogels were also probed for their mechanical properties. Gels were formed for each of the three concentrations, and rheological measurements were obtained. The higher values for the storage modulus over the loss modulus indicated that all three concentrations were in fact hydrogels (Fig. 2). At 1 rad/s, the values for the storage and loss moduli increased in conjunction with the higher concentrations of the skeletal muscle ECM hydrogel. Statistical analyses for these values yielded significant differences for all comparisons, excluding the 4 mg/mL and 6 mg/mL ECM hydrogels for the loss modulus. These results were expected based on the increased amount of ECM proteins associated with the higher concentrations, and the higher packing density observed in the SEM images also supported these outcomes. Compared to other hydrogels for regenerative medicine applications, the mechanical properties are similar to decellularized ECM hydrogels from other tissue sources but are also significantly weaker than materials with cross-linking.[45-50] The decellularized ECM hydrogels used in this study are also known to be extremely weak relative to native muscle; however, beneficial effects have still been observed despite the lack of mechanical strength.[7]

In addition to the storage and loss moduli measurements, viscosity data was also collected on a rheometer (Fig. 3). Viscosity measurements were performed with the liquid form of the ECM hydrogels to ensure each concentration would retain its shear thinning properties, and therefore injectability. All three ECM hydrogels were determined to be shear thinning since the viscosity of the materials decreased with increasing shear rate. The viscosities of the 4 and 6 mg/mL ECM hydrogels were similar, particularly in the 0.1 to 1 Hz shear rate range. However, the viscosity measurements for the 8 mg/mL ECM hydrogel were higher than the other two concentrations. Although all three ECM hydrogels were shear thinning, the increased viscosity with the 8 mg/mL could contribute to some difficulty with injecting these ECM hydrogels through high gauge needles.

3.2 Material spreading and retention

Increased concentration and enhanced mechanical properties are expected to increase material retention and delay degradation, but it was necessary to confirm this *in vivo*. When intramuscularly injecting the three skeletal muscle ECM hydrogels, the increasing concentration affected the ease of injection. All three concentrations were successfully injected, but for the 4 mg/mL hydrogel, the material was more likely to leak out of the tissue following the injection due to the low viscosity. Moreover, the resistance was higher for injecting the 8 mg/mL hydrogel; therefore, the timing of the injection was slightly longer (~45 seconds) compared to the other injections.

At the time of harvesting the muscles at 1 and 2 weeks post-injection, some dye-labelled material was immediately visible near or at the surface of the gracilis muscles. However, the distribution and retention of the skeletal muscle ECM hydrogels could only be visualized with fluorescence microscopy (Fig. 4A). Previous studies identified complete degradation of the 6 mg/mL skeletal muscle ECM hydrogel by 3 weeks;[6] therefore, shorter time points were used to capture the initial degradation process. At 1 week post-injection, the ECM hydrogel was distributed throughout all of the sampled regions with all three concentrations having similar amounts of hydrogel present at each location (data not shown). However, the majority of the material for all three concentrations was more localized to the distal region of the muscle. Boluses of the material were seen for all three concentrations, but the spreading from these boluses varied amongst the concentrations. For the 4 and 6 mg/mL ECM hydrogels, the material spread more readily between the muscle fascicles. However, the 8 mg/mL ECM hydrogel spread less readily and instead remained localized to the surfaces of the muscles. Since this localization was consistently observed in the 8 mg/mL samples, it

likely resulted from the material being forced out of the muscle along the original track of the needle. Therefore, it is hypothesized the 8 mg/mL ECM hydrogel was too viscous to spread significantly throughout the muscle.

Although the retention of the three concentrations was similar at 1 week post-injection, differences were seen at 2 weeks post-injection. Based on the fluorescence microscopy images (Fig. 4A), the 4 and 6 mg/mL ECM hydrogels still maintained some intrafascicular spreading, but the boluses of material were smaller compared to the 1 week post-injection images. Comparably, the boluses of the 8 mg/mL ECM hydrogel on the surface of the gracilis muscle had decreased in size, but only marginally. To quantify these observations at 2 weeks post-injection, the area covered by the dye-labelled ECM hydrogels was calculated relative to the total area of the tissue sections at each location (Fig. 4B). For the total percentage of material over the 13 sampled regions, the most material (although

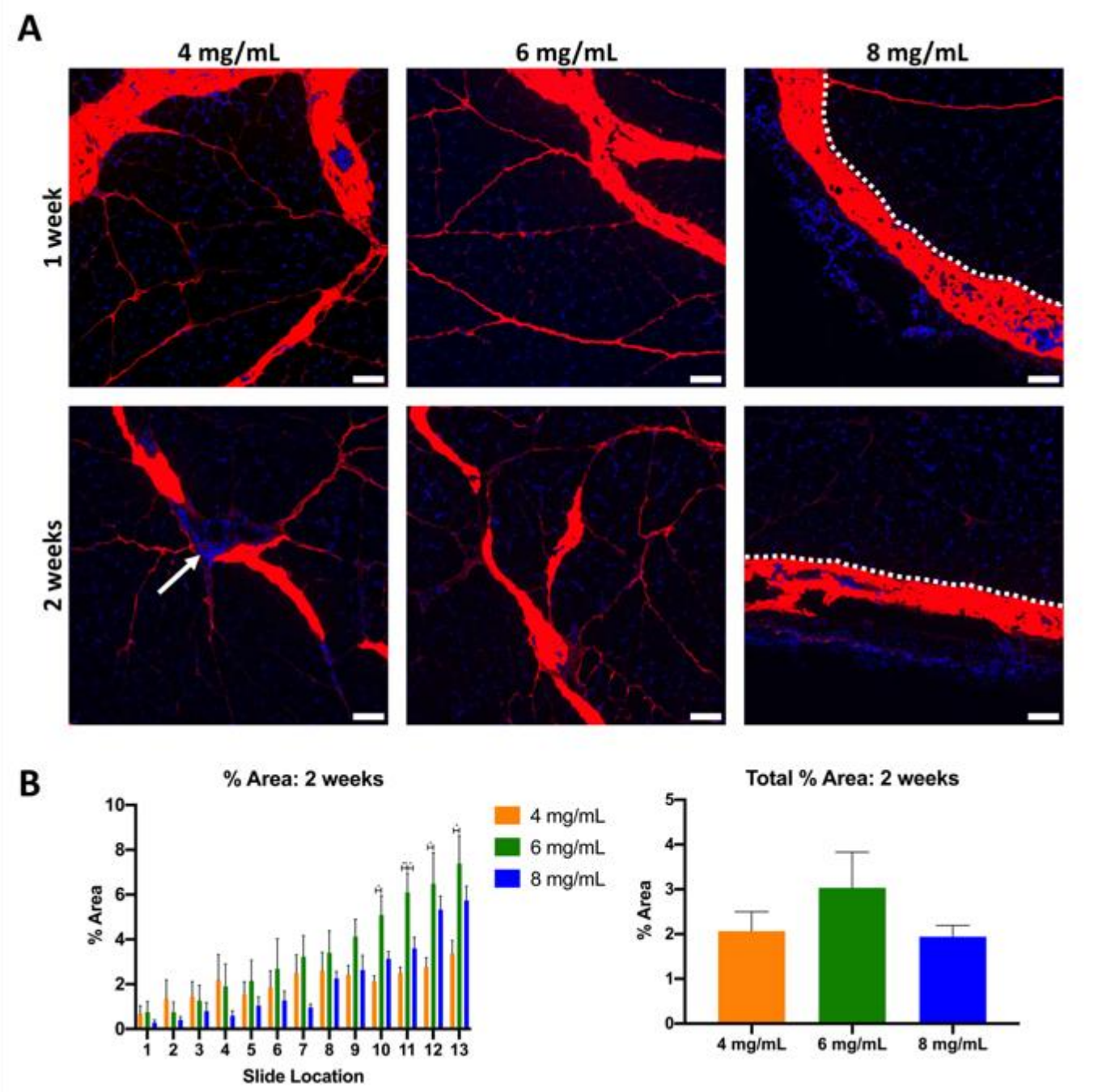

Fig. 4 (A) Dye-labelled skeletal muscle ECM hydrogels (red) were injected into the gracilis muscles of healthy rats. The material was distributed along the length of the muscle, but the 4 mg/mL and 6 mg/mL hydrogels had the highest degree of spreading with material visualized in the intrafascicular space, whereas the 8 mg/mL ECM hydrogel was mostly localized to the surface of the muscle. By 2 weeks post-injection, the 4 mg/mL and 8 mg/mL ECM hydrogels had lower retention than the 6 mg/mL ECM hydrogel, and the 4 mg/mL ECM hydrogel had regions of hypercellularity (nuclei in blue) present within the material, likely indicative of active degradation. (B) The material distribution and retention were quantified at 2 weeks post-injection (n = 4/concentration) with 1 being the most proximal region and 13 being the most distal region. White arrow represents a region of degradation, while the dotted lines indicate the surface of the gracilis muscle according to adjacent H&E images. Scale bar is 100 µm. *$p < 0.05$, **$p < 0.01$. Data are ± SEM.

not statistically significant) was retained with the 6 mg/mL ECM hydrogel at 3.03 ± 0.80%, while the 4 mg/mL and 8 mg/mL ECM hydrogels had 2.07 ± 0.43% and 1.94 ± 0.25% retained, respectively. There were noticeable and significant differences between each material concentration at different locations within the muscle, further indicating differences in spreading. Similar amounts of the 4 mg/mL ECM hydrogel were visible throughout the muscle at each location, but the large boluses of material were not as prevalent in the distal locations. This was likely due to the 4 mg/mL ECM hydrogel being degraded more rapidly since areas of hypercellularity were seen within the material, which overlapped with decreased signal from the dye-labelled material. Compared to the 4 mg/mL ECM hydrogel, the 6 mg/mL hydrogel had similar amounts of material in the proximal locations, but significantly larger amounts of the 6 mg/mL ECM hydrogel were still present in the distal locations at 2 weeks post-injection. The large boluses of 8 mg/mL ECM hydrogel were slightly smaller at 2 weeks post-injection with more holes present, likely indicating some degree of degradation. While only a small amount of dye was used (approximately 10 available amines per dye molecule), there is the possibility that a small fraction of free dye remains unbound or is released upon material degradation; however, we previously showed this dye-labelling method correlated well with presence of ECM hydrogels in H&E stained sections.[41]

Since the material spreading and retention was evaluated in healthy hindlimbs of rats, the inflamed, ischemic environment was not fully recapitulated. However, these results still provided valuable information to determine which concentration may produce enhanced therapeutic outcomes. The 8 mg/mL ECM hydrogel had poor spreading, which may limit its therapeutics effects. Conversely, the 4 mg/mL ECM hydrogel spread well throughout the muscle, thereby potentially affecting more of the muscle. However, the 4 mg/mL ECM hydrogel leaked out of the muscle to a greater extent than the other concentrations, and the material was more degraded than the 6 mg/mL ECM hydrogel at 2 weeks post-injection. In contrast, the 6 mg/mL ECM hydrogel was injected with relative ease while avoiding leakage, spreading extensively throughout the muscle, and degrading at a slower rate.

3.3 Dose optimization

A previous study yielded a significant improvement in blood perfusion with a 6 mg/mL skeletal muscle ECM hydrogel compared to saline, but an optimal concentration was not identified.[7] We therefore wanted to compare three ECM hydrogel concentrations to evaluate changes in blood perfusion recovery. By utilizing the same species and surgical procedure as the initial efficacy studies for the 6 mg/mL skeletal muscle ECM hydrogel, this allowed for the known therapeutic effects of the 6 mg/mL ECM hydrogel to be confirmed and then compared to the unestablished results from the 4 and 8 mg/mL ECM hydrogels. The dosing optimization served as a pilot experiment to evaluate trends related to increases in blood perfusion; therefore, the study was not powered due to the high number of animals that would be required to evaluate the expected small changes in perfusion between the multiple groups.

Relative to the injections performed in the healthy, non-ischemic rats, the ECM hydrogel injections were similar in the ischemic

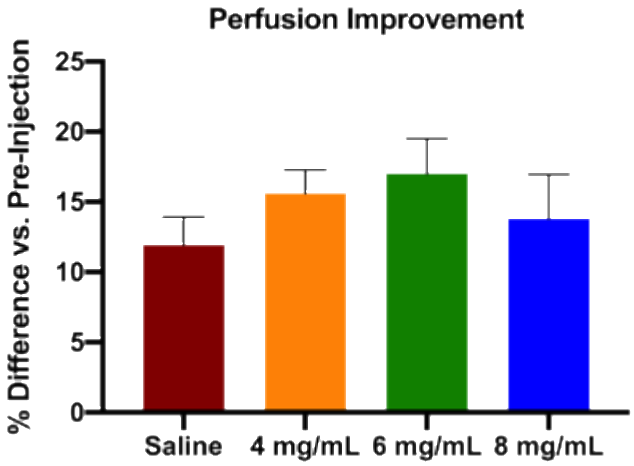

Fig. 5 Blood perfusion measurements were recorded using LASCA imaging. The 6 mg/mL ECM hydrogel (n=8) yielded the largest improvement in blood perfusion relative to the other two concentrations (n=7) and the saline control (n=8). Improvements in perfusion were calculated using the difference between day 35 post- injection versus pre-injection (day -2). Data are mean ± SEM.

muscles with comparable leakage occurring, but the surgical incision offered a reliable landmark for guaranteeing similar injection sites across all of the animals. Immediately post-hindlimb ischemia surgery, the blood perfusion values for all experimental groups averaged at 33.80 ± 1.33%, and by day -2 post-injection, the average of the blood perfusion values had already increased to 56.85 ± 1.43%. At the conclusion of the study, the differences between the perfusion values at day 35 and pre-injection (day -2) were calculated (Fig. 5). The 6 mg/mL ECM hydrogel (n=8) ultimately yielded the highest improvement in blood perfusion at 16.98 ± 2.50% compared to the saline control (n=8) at 11.90 ± 2.01%. The 4 mg/mL (n=7) and 8 mg/mL (n=7) ECM hydrogels also trended higher over the saline control at 15.58 ± 1.71% and 13.79 ± 3.16%, respectively, but to a lesser degree compared to the 6 mg/mL ECM hydrogel. The lack of improvement observed from the 4 and 8 mg/mL concentrations were hypothesized to be a result of the material spreading patterns and degradation rates as described above. Although the 4 mg/mL ECM hydrogel shared a similar spreading pattern to the 6 mg/mL ECM hydrogel in healthy gracilis muscles, the increased presence of inflammatory cells due to the hindlimb ischemia surgery could have amplified the degradation rate. In addition, the lower viscosity of the 4 mg/mL ECM hydrogel resulted in more material leaking from the injection site. With a weaker structure and fewer ECM proteins to degrade, the 4 mg/mL ECM hydrogel likely degraded before beneficial processes, such as neovascularization, could be initiated. For the 8 mg/mL ECM hydrogel, the restricted spreading and slower degradation of the material likely limited an arteriogenic response to a smaller area of the muscle, which resulted in smaller improvements in blood perfusion relative to the 6 mg/mL ECM hydrogel.

Other researches have also demonstrated the importance of material spreading and degradation rates for eventual *in vivo* efficacy.[51-53] The effects of material spreading are not well documented in skeletal muscle applications, but, for other therapeutic targets, such as the heart, poor material spreading can lead to dangerous outcomes like causing arrhythmias.[53] In the case of skeletal muscle, large boluses of an ECM hydrogel would likely be

more difficult for cells to fully infiltrate and degrade, which could subsequently impede or prevent regeneration. Degradation rates have been more extensively studied both *in vitro* and *in vivo* for several decellularized ECM materials.[41,48,54,55] These researchers have demonstrated how highly crosslinked or dense biomaterials attenuate cell migration, and the mechanical properties of these materials dissipate quickly upon degradation. As a result, optimal physical properties and biochemical cues are paramount to ensure cells can infiltrate and subsequently remodel a biomaterial to form native tissue in the injured region.

All of the ECM hydrogels yielded higher improvements in blood perfusion over the saline control when calculating the differences between the perfusion values at day 35 versus pre-injection (day -2). As mentioned above, this study was intended to identify trends amongst the three concentrations; therefore, no significant differences were detected between the experimental groups ($p = 0.101$). Nonetheless, the 6 mg/mL ECM hydrogel yielded the highest improvement in blood perfusion, whereas the 4 mg/mL and 8 mg/mL ECM hydrogels produced marginal improvements over the saline control. These results indicated that 6 mg/mL was the optimal concentration for performing further validation.

Although hindlimb ischemia models represent the standard for investigating PAD, the model has several limitations. To achieve a sufficiently severe model to circumvent the inherent regeneration of young rats, the hindlimb ischemia surgery involved ligation and excision of the femoral artery and vein; however, other researchers often excise only the femoral artery or only utilize ligation for one or both of the vessels. Furthermore, therapeutic injections are typically performed immediately at the time of surgery when there is an intense acute inflammatory response due to the rapid recovery of these models, which does not model the chronic condition of PAD patients. We therefore chose to use the ligation and excision model for both vessels, which would allow us to perform injections one-week after ischemia surgery to avoid performing injections during this acute inflammatory response. Regardless, this surgical approach and the majority of other hindlimb ischemia surgeries fail to mimic the gradual occlusion of vessels over time in PAD patients, which is a known limitation in the field.

3.4 Efficacy in aged mice

The hindlimb ischemia model has many limitations, but the model can be improved with the use of more representative animals. Young animals, particularly rodents, are known to possess remarkable regenerative capabilities regardless of any interventions; however, these animals are also readily available, much cheaper to use, and still represent the standard in the field. Many pre-clinical studies for PAD have relied on young animal models to evaluate therapies, but the limited success in humans could be attributed to the use of inadequate animal models. The dose optimization study was performed with young rats to expand upon previous studies related to the efficacy of the decellularized skeletal muscle ECM hydrogel,[7] and trends were observed with the 6 mg/mL ECM hydrogel, as discussed above. However, we wanted to validate those results with a more relevant animal model to more accurately recapitulate the pathophysiology of PAD patients, who are typically older and suffer from comorbidities.

Researchers have incorporated the use of aged animals for hindlimb ischemia studies, and those animals have failed to regenerate as readily, which more accurately mimics the PAD patient population.[22,56-59] In addition, when evaluating therapeutics including growth factors, cells, and biomaterials, the interventions did not perform as effectively in aged animals.[31-38] Consequently, after confirming 6 mg/mL was the optimal concentration, we wanted to validate its efficacy in a more relevant animal model of PAD. For this experiment, aged mice were used to investigate whether age-related impairments would inhibit increases in perfusion from the administration of the 6 mg/mL ECM hydrogel (Fig. 6). Since aged rats were not readily available, aged mice were instead used.

After performing the hindlimb ischemia surgeries in the mice, some animals developed necrosis in the toes of the ischemic paw,

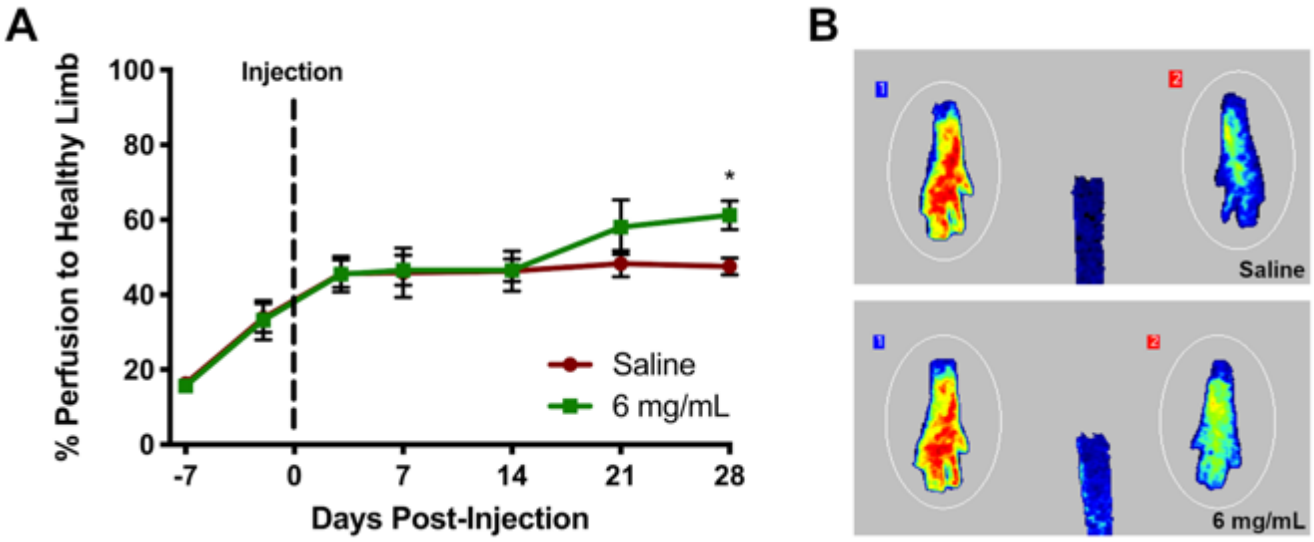

Fig. 6 An aged mouse hindlimb ischemia model (n=6/group) was utilized, and blood perfusion measurements were acquired with LASCA imaging. (A) Significant improvements in blood perfusion values were seen at 28 days post-injection. (B) Representative LASCA images are shown for day 28 post-injection. *$p < 0.05$ according to an unpaired Student's t-test at day 28 post-injection. Data are mean ± SEM.

which was not evident in any of the young rats in previous experiments. The hindlimb ischemia surgeries were also more severe in that the blood perfusion immediately post-surgery was an average of 15.95 ± 0.91% for all of the mice. At day -2 post-injection, the average blood perfusion had only increased to 33.51 ± 3.10%. In addition to the necrosis seen in the mice, the limited improvement in blood perfusion recovery between days 3-14 post-injection in both experimental groups indicated that the hindlimb ischemia surgery was more severe in the aged mice and impaired the natural regenerative process more so than the young rats. At day 21 post-injection, the ECM hydrogel-injected mice began improving more than the saline control. In our previous studies in young rats, we showed the ECM hydrogel increased neovascularization.[6,7] The neovascularization process, which is typically stimulated at ~7 days post-injection, was likely delayed by the aged environment, but by day 28 post-injection, the blood perfusion values for the ECM hydrogel group were significantly higher (Fig. 6A, $p = 0.012$). These results support a previous study in which blood perfusion recovery and increased vessel density arising from the injection of growth factor-loaded alginate gels were increasingly limited in older mice.[38] The saline control reached a blood perfusion level of only 47.50 ± 2.25% at day 28 post-injection, but the ECM hydrogel increased the blood perfusion to 61.24 ± 3.87% (Fig. 6B).

The previous published study, which investigated the 6 mg/mL ECM hydrogel in a young rat hindlimb ischemia model, showed significantly higher perfusion values at 80.21 ± 3.85% compared to the saline control at 69.06 ± 2.63% for day 35 post-injection.[7] Increases in the perfusion values began at day 14 post-injection and reached significance by day 21 for the young rat hindlimb ischemia study,[7] but the aged mice in this study did not show increases in perfusion until day 21 with significance achieved at day 28 post-injection. This delay in the restoration of the blood perfusion may also be attributed to age of the animals since studies have described age-related impairments in important regenerative processes like angiogenesis,[22,23] vasculogenesis,[23] and satellite cell activity.[26-28] The higher perfusion values for the rats relative to the aged mice could indicate impairments resulting from aging or could be associated with species differences. Injecting saline is known to cause an inflammatory response that could initiate some regeneration, but it was unable to increase perfusion beyond day 3 post-injection, or ~47% perfusion, in the aged mice. However, the administration of the 6 mg/mL ECM hydrogel restored the blood perfusion values to a higher value. The aged mice could be a more reliable model for detecting significant differences due to administration of the ECM hydrogels as the limited regeneration more accurately depicts the PAD and CLI patients who may be aged or suffering from other comorbidities that would attenuate normal healing processes.

4. Conclusions

In summary, we have characterized the physical properties of three concentrations of a decellularized skeletal muscle ECM hydrogel and investigated the efficacy of these hydrogels in a hindlimb ischemia model. We demonstrated the importance of evaluating material retention and spreading *in vivo* as it may not change linearly with material concentration. Although the increasing concentrations of the ECM hydrogels corresponded to an increase in viscosity and mechanical strength, the spreading patterns and degradation rates impacted the *in vivo* efficacy, likely a result of differing biochemical cues amongst the various concentrations. The 6 mg/mL ECM hydrogel restored the blood perfusion to the highest value and was identified as the optimal concentration. Efficacy was further demonstrated in an aged mouse hindlimb ischemia model. Significant increases in blood perfusion were observed in the aged mice, which are more representative of the pathophysiology of the patient population. Overall, this study provides further proof-of-concept for the use of decellularized skeletal muscle ECM hydrogels for eventual translation to PAD patients.

Conflicts of interest

K.L. Christman is co-founder, consultant, board member, and holds equity interest in Ventrix, Inc.

Acknowledgements

This work was supported by the California Institute for Regenerative Medicine (TRAN1-09814). MJH was supported by a National Institutes of Health pre-doctoral fellowship (1F31HL132584). We would like to thank Martin Spang for performing the scanning electron microscopy at the San Diego Nanotechnology Infrastructure (SDNI) of UCSD, a member of the National Nanotechnology Coordinated Infrastructure (NNCI), which is supported by the National Science Foundation (ECCS-1542148).

References

1 H. Lawall, P. Bramlage and B. Amann, *Thromb Haemost*, 2010, **103**, 696-709.
2 J. Dormandy, L. Heeck and S. Vig, *Semin Vasc Surg*, 1999, **12**, 142-147.
3 M. Schillinger, S. Sabeti, P. Dick, J. Amighi, W. Mlekusch, O. Schlager, C. Loewe, M. Cejna, J. Lammer and E. Minar, *Circulation*, 2007, **115**, 2745-2749.
4 J. L. Ungerleider and K. L. Christman, *Stem Cells Transl Med*, 2014, **3**, 1090-1099.
5 M. J. Hernandez and K. L. Christman, *JACC Basic Transl Sci*, 2017, **2**, 212-226.
6 J. A. Dequach, J. E. Lin, C. Cam, D. Hu, M. A. Salvatore, F. Sheikh and K. L. Christman, *Eur Cell Mater*, 2012, **23**, 400-412; discussion 412.
7 J. L. Ungerleider, T. D. Johnson, M. J. Hernandez, D. I. Elhag, R. L. Braden, M. Dzieciatkowska, K. G. Osborn, K. C. Hansen, E. Mahmud and K. L. Christman, *JACC: Basic to Translational Science*, 2016, **1**, 32-44.
8 V. S. Chekanov, R. Rayel, V. Nikolaychik, N. Kipshidze, I. Baibekov, P. Karakozov, T. Bajwa and M. Akhtar, *J Card Surg*, 2002, **17**, 502-511; discussion 512.
9 C. E. Luyt, A. Meddahi-Pelle, B. Ho-Tin-Noe, S. Colliec-Jouault, J. Guezennec, L. Louedec, H. Prats, M. P. Jacob, M. Osborne-Pellegrin, D. Letourneur and J. B. Michel, *J Pharmacol Exp Ther*, 2003, **305**, 24-30.

10 G. S. Hussey, J. L. Dziki and S. F. Badylak, *Nature Reviews Materials*, 2018, **3**, 159-173.
11 R. P. Mecham, *Curr Protoc Cell Biol*, 2012, **Chapter 10**, Unit 10 11.
12 F. Li, W. Li, S. Johnson, D. Ingram, M. Yoder and S. Badylak, *Endothelium*, 2004, **11**, 199-206.
13 S. F. Badylak, K. Park, N. Peppas, G. Mccabe and M. Yoder, *Exp Hematol*, 2001, **29**, 1310-1318.
14 S. Numata, T. Fujisato, K. Niwaya, H. Ishibashi-Ueda, T. Nakatani and S. Kitamura, *J Heart Valve Dis*, 2004, **13**, 984-990.
15 T. Zantop, T. W. Gilbert, M. C. Yoder and S. F. Badylak, *J Orthop Res*, 2006, **24**, 1299-1309.
16 E. Rieder, A. Nigisch, B. Dekan, M. T. Kasimir, F. Muhlbacher, E. Wolner, P. Simon and G. Weigel, *Biomaterials*, 2006, **27**, 5634-5642.
17 J. E. Reing, L. Zhang, J. Myers-Irvin, K. E. Cordero, D. O. Freytes, E. Heber-Katz, K. Bedelbaeva, D. Mcintosh, A. Dewilde, S. J. Braunhut and S. F. Badylak, *Tissue Eng Part A*, 2009, **15**, 605-614.
18 A. J. Beattie, T. W. Gilbert, J. P. Guyot, A. J. Yates and S. F. Badylak, *Tissue Eng Part A*, 2009, **15**, 1119-1125.
19 N. Rao, G. Agmon, M. T. Tierney, J. L. Ungerleider, R. L. Braden, A. Sacco and K. L. Christman, *ACS Nano*, 2017, **11**, 3851-3859.
20 L. H. Eraso, E. Fukaya, E. R. Mohler, 3rd, D. Xie, D. Sha and J. S. Berger, *Eur J Prev Cardiol*, 2014, **21**, 704-711.
21 M. D. Grounds, *Ann N Y Acad Sci*, 1998, **854**, 78-91.
22 A. Rivard, J. E. Fabre, M. Silver, D. Chen, T. Murohara, M. Kearney, M. Magner, T. Asahara and J. M. Isner, *Circulation*, 1999, **99**, 111-120.
23 T. Shimada, Y. Takeshita, T. Murohara, K. Sasaki, K. Egami, S. Shintani, Y. Katsuda, H. Ikeda, Y. Nabeshima and T. Imaizumi, *Circulation*, 2004, **110**, 1148-1155.
24 B. M. Carlson, *J Gerontol A Biol Sci Med Sci*, 1995, **50 Spec No**, 96-100.
25 O. Delbono, *Aging Cell*, 2003, **2**, 21-29.
26 I. M. Conboy, M. J. Conboy, A. J. Wagers, E. R. Girma, I. L. Weissman and T. A. Rando, *Nature*, 2005, **433**, 760-764.
27 A. S. Brack, M. J. Conboy, S. Roy, M. Lee, C. J. Kuo, C. Keller and T. A. Rando, *Science*, 2007, **317**, 807-810.
28 F. Le Grand and M. A. Rudnicki, *Curr Opin Cell Biol*, 2007, **19**, 628-633.
29 B. M. Carlson and J. A. Faulkner, *American Journal of Physiology - Cell Physiology*, 1989, **256**, C1262-C1266.
30 G. Goldspink, K. Fernandes, P. E. Williams and D. J. Wells, *Neuromuscul Disord*, 1994, **4**, 183-191.
31 J. Yu, L. Lei, Y. Liang, L. Hinh, R. P. Hickey, Y. Huang, D. Liu, J. L. Yeh, E. Rebar, C. Case, K. Spratt, W. C. Sessa and F. J. Giordano, *FASEB J*, 2006, **20**, 479-481.
32 S. Sugihara, Y. Yamamoto, T. Matsuura, G. Narazaki, A. Yamasaki, G. Igawa, K. Matsubara, J. Miake, O. Igawa, C. Shigemasa and I. Hisatome, *Mech Ageing Dev*, 2007, **128**, 511-516.
33 Y. Zhuo, S. H. Li, M. S. Chen, J. Wu, H. Y. Kinkaid, S. Fazel, R. D. Weisel and R. K. Li, *J Thorac Cardiovasc Surg*, 2010, **139**, 1286-1294, 1294 e1281-1282.
34 M. Palladino, I. Gatto, V. Neri, S. Straino, M. Silver, A. Tritarelli, A. Piccioni, R. C. Smith, E. Gaetani, D. W. Losordo, F. Crea, M. Capogrossi and R. Pola, *Mol Ther*, 2011, **19**, 658-666.
35 W. Fan, C. Li, X. Qin, S. Wang, H. Da, K. Cheng, R. Zhou, C. Tong, X. Li, Q. Bu, C. Li, Y. Han, J. Ren and F. Cao, *Aging Cell*, 2013, **12**, 32-41.
36 R. Madonna, D. A. Taylor, Y. J. Geng, R. De Caterina, H. Shelat, E. C. Perin and J. T. Willerson, *Circ Res*, 2013, **113**, 902-914.
37 V. A. Kumar, Q. Liu, N. C. Wickremasinghe, S. Shi, T. T. Cornwright, Y. Deng, A. Azares, A. N. Moore, A. M. Acevedo-Jake, N. R. Agudo, S. Pan, D. G. Woodside, P. Vanderslice, J. T. Willerson, R. A. Dixon and J. D. Hartgerink, *Biomaterials*, 2016, **98**, 113-119.
38 E. M. Anderson, E. A. Silva, Y. Hao, K. D. Martinick, S. A. Vermillion, A. G. Stafford, E. G. Doherty, L. Wang, E. J. Doherty, P. M. Grossman and D. J. Mooney, *J Vasc Res*, 2017, **54**, 288-298.
39 J. L. Ungerleider, T. D. Johnson, N. Rao and K. L. Christman, *Methods*, 2015, **84**, 53-59.
40 M. J. Hernandez, G. E. Yakutis, E. I. Zelus, R. C. Hill, M. Dzieciatkowska, K. C. Hansen and K. L. Christman, *Methods*, 2019.
41 J. W. Wassenaar, R. L. Braden, K. G. Osborn and K. L. Christman, *J Mater Chem B*, 2016, **4**, 2794-2802.
42 M. Roustit, C. Millet, S. Blaise, B. Dufournet and J. L. Cracowski, *Microvasc Res*, 2010, **80**, 505-511.
43 J. Senarathna, A. Rege, N. Li and N. V. Thakor, *IEEE Rev Biomed Eng*, 2013, **6**, 99-110.
44 T. D. Johnson, S. Y. Lin and K. L. Christman, *Nanotechnology*, 2011, **22**, 494015.
45 D. O. Freytes, J. Martin, S. S. Velankar, A. S. Lee and S. F. Badylak, *Biomaterials*, 2008, **29**, 1630-1637.
46 J. L. Vanderhooft, M. Alcoutlabi, J. J. Magda and G. D. Prestwich, *Macromol Biosci*, 2009, **9**, 20-28.
47 C. Yan and D. J. Pochan, *Chem Soc Rev*, 2010, **39**, 3528-3540.
48 J. M. Singelyn and K. L. Christman, *Macromol Biosci*, 2011, **11**, 731-738.
49 M. T. Wolf, K. A. Daly, E. P. Brennan-Pierce, S. A. Johnson, C. A. Carruthers, A. D'amore, S. P. Nagarkar, S. S. Velankar and S. F. Badylak, *Biomaterials*, 2012, **33**, 7028-7038.
50 A. R. Massensini, H. Ghuman, L. T. Saldin, C. J. Medberry, T. J. Keane, F. J. Nicholls, S. S. Velankar, S. F. Badylak and M. Modo, *Acta Biomater*, 2015, **27**, 116-130.
51 K. Y. Lee, K. H. Bouhadir and D. J. Mooney, *Biomaterials*, 2004, **25**, 2461-2466.
52 J. A. Burdick, C. Chung, X. Jia, M. A. Randolph and R. Langer, *Biomacromolecules*, 2005, **6**, 386-391.
53 S. L. Suarez, A. A. Rane, A. Munoz, A. T. Wright, S. X. Zhang, R. L. Braden, A. Almutairi, A. D. Mcculloch and K. L. Christman, *Acta Biomater*, 2015, **26**, 13-22.
54 R. D. Record, D. Hillegonds, C. Simmons, R. Tullius, F. A. Rickey, D. Elmore and S. F. Badylak, *Biomaterials*, 2001, **22**, 2653-2659.
55 A. Costa, J. D. Naranjo, N. J. Turner, I. T. Swinehart, B. D. Kolich, S. A. Shaffiey, R. Londono, T. J. Keane, J. E. Reing, S. A. Johnson and S. F. Badylak, *Biomaterials*, 2016, **108**, 81-90.
56 M. Bosch-Marce, H. Okuyama, J. B. Wesley, K. Sarkar, H. Kimura, Y. V. Liu, H. Zhang, M. Strazza, S. Rey, L. Savino, Y. F. Zhou, K. R. Mcdonald, Y. Na, S. Vandiver, A. Rabi, Y. Shaked, R. Kerbel, T. Lavallee and G. L. Semenza, *Circ Res*, 2007, **101**, 1310-1318.
57 T. S. Westvik, T. N. Fitzgerald, A. Muto, S. P. Maloney, J. M. Pimiento, T. T. Fancher, D. Magri, H. H. Westvik, T. Nishibe, O. C. Velazquez and A. Dardik, *J Vasc Surg*, 2009, **49**, 464-473.
58 J. S. Wang, X. Liu, Z. Y. Xue, L. Alderman, J. U. Tilan, R. Adenika, S. E. Epstein and M. S. Burnett, *Chin Med J (Engl)*, 2011, **124**, 1075-1081.
59 J. E. Faber, H. Zhang, R. M. Lassance-Soares, P. Prabhakar, A. H. Najafi, M. S. Burnett and S. E. Epstein, *Arterioscler Thromb Vasc Biol*, 2011, **31**, 1748-1756.

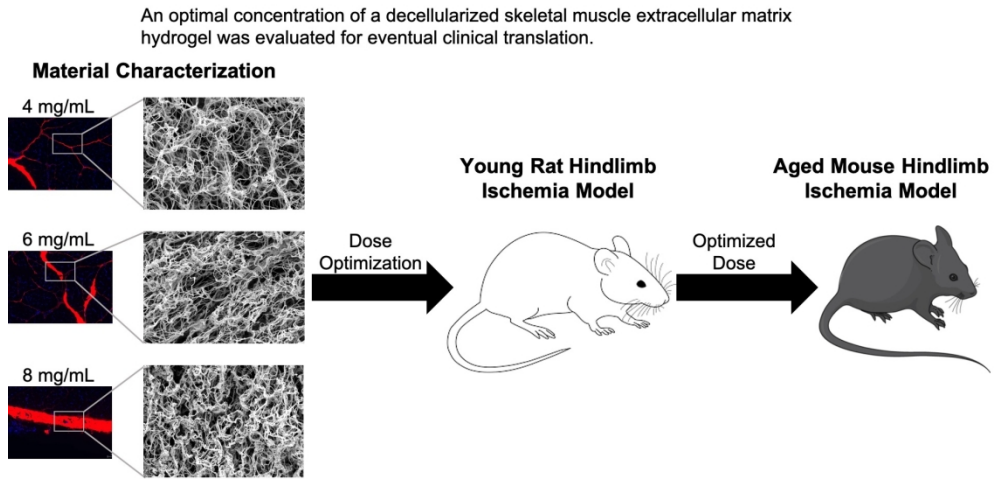

342x164mm (144 x 144 DPI)